

Particle-core coupling for heavy odd-odd and odd-even Sb nuclei: A shell model approach

J. Sau and K. Heyde*

Institut de Physique Nucléaire and I N2 P3, Université Claude Bernard Lyon-1, 43 Bd du 11 Novembre 1918-F 69622 Villeurbanne Cedex, France

(Received 10 December 1980)

Particle-core coupling calculations on heavy odd-odd and odd-even Sb nuclei have been carried out, starting from a shell-model description. Starting from a description of the core system (Sn nuclei) and a multipole-multipole proton-neutron interaction, we have derived particle-core coupling matrix elements (applicable to odd-mass as well as to odd-odd nuclei). Detailed calculations have been carried out for ^{132,130,129}Sb. In the latter case, extensive comparison is made with macroscopic particle-core coupling calculations.

[NUCLEAR STRUCTURE Particle-core coupling, shell-model approach. Application to ^{132, 130, 129}Sb.]

I. INTRODUCTION

In describing nuclei where the number of valence nucleons is not far from a closed shell configuration ($\pm 1, \pm 2, \pm 3, \pm 4$), specific nucleon configurations remain such as to make a description in terms of collective excitations difficult or impossible. This happens to be the case for the heavy Sn nuclei¹⁻⁴ near the $Z = 50, N = 82$ doubly-closed shell configuration: ^{128, 129, 130}Sn. In trying to couple the extra proton in Sb nuclei with the excitations of the underlying core, one observes large deviations from the macroscopic particle-core coupling mechanism.⁵⁻¹² Very specific one-proton- n -neutron-hole excitations remain. In order to attempt a complete description of the core system as well as of the particle-core coupled states, one has to start from a shell-model approach.

In Sec. II, we derive the basic equations for the shell-model approach to particle-core coupling, being able to describe odd-odd as well as odd-even nuclei. A connection with the macroscopic particle-core coupling matrix element is pointed out. Finally, in Sec. III, application to the 1p-3h and 1p-4h nuclei of Sb will be made and comparison

with the macroscopic particle-core coupling (in the latter case of ¹²⁹Sb) will be carried out.

II. METHODS AND SHELL-MODEL INGREDIENTS

A. Methods

In an earlier article,¹³ we derived a general expression for calculating matrix elements describing an interacting system of n_i protons and n_k neutrons. Let us call $|C_i J_i M_i\rangle$ ($|C_k J_k M_k\rangle$) the resulting wave function of n_i protons (n_k neutrons), C_i (C_k) being all other quantum numbers necessary to label the wave function uniquely. These wave functions are obtained by diagonalizing for the particular nuclei with n_i protons (n_k neutrons) the residual proton-proton (neutron-neutron) interaction. We will not go into the details of the construction of the orthonormal basis states,¹⁴ nor of the explicit construction of energy matrices which, for $n_i, n_k \geq 4$, can become a very cumbersome and time consuming task.¹⁵ Some pertinent results for ¹²⁹Sn will be discussed in Sec. II B.

The proton-neutron residual interaction V_{pn} results in the following matrix element¹³:

$$\langle C'_i J'_i, C'_k J'_k; J | V_{pn} | C_i J_i, C_k J_k; J \rangle = \sum_{\substack{J'_i \\ p p', n n'}} U((p'p)(n'n)J') (-1)^{J_i + J_k + J - J'} \begin{Bmatrix} J_k & J' & J_k \\ J_i & J & J_i \end{Bmatrix} \times \langle C'_k J'_k || (p'p) J' || C_i J_i \rangle \langle C'_i J'_i || (h'h) J' || C_k J_k \rangle. \tag{2.1}$$

In the particular case n_i proton particles (p, p') and n_k neutron holes (h', h), we make use of the following definitions:

$$U((p'p)(h'h), J') = \hat{J}'^2 \sum_{J_1} \hat{J}_1^2 (-1)^{J_p + J_{h'} + J' + J_1} \begin{Bmatrix} j_{p'} & J_1 & j_{h'} \\ j_h & J' & j_p \end{Bmatrix} \langle p' h'^{-1} J_1 | V_{pn} | p h^{-1} J_1 \rangle, \tag{2.2}$$

where $\langle p'h'^{-1}; J_1 | V_{pn} | ph^{-1}; J_1 \rangle$ is the matrix element of the proton particle neutron hole interaction, and

$$\langle C_i' J_i' || (p'p) J' || C_i J_i \rangle \equiv \frac{1}{j_i'} \langle C_i' J_i' || [a_p^+, a_p]^{J'} || C_i J_i \rangle, \quad (2.3)$$

$[a_p^+ a_p]^\lambda$ meaning the usual vector coupling.

In this paper we have restricted the V_{pn} interaction to a sum of multipole-multipole forces in order to allow for a fruitful comparison with the more macroscopic approach of the unified model.

Then with

$$V_{pn} = \sum_\lambda \chi_\lambda Q_\lambda(\vec{r}_p) \cdot Q_\lambda(\vec{r}_n), \quad (2.4)$$

with

$$Q_{\lambda\mu}(\vec{r}) = \left[\left(\frac{m\omega}{\hbar} \right)^{1/2} r \right]^\lambda Y_{\lambda\mu},$$

one gets easily by a straightforward calculation

$$\begin{aligned} \langle p', C_{k'} J_{k'}; JM | V_{pn} | p, C_k J_k; JM \rangle \\ = \sum_\lambda \chi_\lambda (-1)^{j_p + J_k + J} \begin{Bmatrix} J_k & \lambda & J_{k'} \\ j_p & J & j_p \end{Bmatrix} \\ \times \langle p' || Q_\lambda || p \rangle \langle C_k' J_k' || Q_\lambda || C_k J_k \rangle. \end{aligned} \quad (2.5)$$

Expression (2.5) is completely equivalent with the macroscopic particle-core matrix element. The core matrix elements (2.5), however, are defined in terms of their shell-model description, whereas in the macroscopic vibrational model, core matrix elements are related to boson coefficients of fractional parentage (cfp's).

B. Parameters, results for Sn nuclei

Application of the 2h, 3h, and 4h nuclei $^{130, 129, 128}\text{Sn}$ has been carried out. Here, the complete space of neutron hole states, i.e., $2d_{3/2}^{-1}$, $3s_{1/2}^{-1}$, $1h_{11/2}^{-1}$, $2d_{5/2}^{-1}$, and $1g_{7/2}^{-1}$ is taken into account. The force considered was a Gaussian interaction with spin exchange admixture, as used already for this particular mass region with considerable success.^{6, 16-20} The force strength, exchange admixture, and neutron single-particle energies are given in Table I.

In discussing the pertinent results for ^{129}Sn , one immediately observes a clear separation between the three lowest states $J_i^\pi = \frac{3}{2}_1^+$, $\frac{1}{2}_1^+$, $\frac{1}{2}_1^+$, and the next higher-lying group of 3 hole states (Fig. 1). In correlating the wave functions for these three lowest states with the $J^\pi = 0^+$ ^{130}Sn ground state wave function (described within the same configuration space as $0.65|2d_{3/2}^{-2}; 0^+\rangle + 0.40|3s_{1/2}^{-2}; 0^+\rangle - 0.58|1h_{11/2}^{-2}; 0^+\rangle$), a direct product representation

$$|JM\rangle \cong |j^{-1}\rangle \otimes |0_1^+, ^{130}\text{Sn}\rangle \delta_{jJ}, \quad (2.6)$$

TABLE I. The parameters for the proton-proton, neutron-neutron, and proton-neutron interactions as well as the proton single-particle and neutron single-hole energies. For the nucleus ^{129}Sn we have used $\tilde{\epsilon}_{1h_{11/2}} = 0.20$ MeV and $\tilde{\epsilon}_{3s_{1/2}} = 0.30$ MeV.

| | Proton | | Neutron |
|------------------------|------------------------------------|--------------------------------|---------|
| $\epsilon_{1s_{1/2}}$ | 0.0 | $\tilde{\epsilon}_{2d_{3/2}}$ | 0.0 |
| $\epsilon_{2d_{5/2}}$ | 1.0 | $\tilde{\epsilon}_{3s_{1/2}}$ | 0.3 |
| $\epsilon_{1h_{11/2}}$ | 2.0 | $\tilde{\epsilon}_{1h_{11/2}}$ | 0.4 |
| $\epsilon_{2d_{3/2}}$ | 2.4 | $\tilde{\epsilon}_{1g_{7/2}}$ | 2.4 |
| $\epsilon_{3s_{1/2}}$ | 2.0 | $\tilde{\epsilon}_{2d_{5/2}}$ | 2.8 |
| V_0 | 39 | V_0 | -39 |
| t | +0.2 | t | +0.2 |
| | $V_1 = -84$ (MeV fm ³) | | |
| | $t' = 5$ | | |

serves as a very good approximation to these wave functions. Comparison with the scarce amount of experimental data is not very compelling,^{2, 4} although a gap between the three low-lying $J_i^\pi = \frac{3}{2}_1^+$, $\frac{1}{2}_1^+$, $\frac{1}{2}_1^+$ levels and the other states starting from $E_x \cong 1$ MeV reproduces the experimental situation well. We have also calculated the reduced $E2$ core matrix elements $\langle J_i || M(E2) || J_j \rangle$ between the lowest-lying ($E_x \lesssim 1.5$ MeV) levels in order to obtain information on the $E2$ collective structure within the space of 3h excitations. From these results (Table II), one clearly observes strong $E2$ reduced matrix elements connecting the $J_i^\pi = \frac{3}{2}_2^+$, $\frac{5}{2}_1^+$, $\frac{1}{2}_2^+$, $\frac{7}{2}_1^+$ states with the $J_j^\pi = \frac{3}{2}_1^+$ ground state, pointing towards a relation within the more macroscopic approach of a hole-quadrupole vibrational $|2d_{3/2}^{-1} \otimes 2_1^+(^{130}\text{Sn})\rangle$ configuration for the former states. Moreover, the $J_i^\pi = \frac{3}{2}_3^+$, $\frac{5}{2}_2^+$ states are strongly connected to the first excited $J_j^\pi = \frac{1}{2}_1^+$ level, pointing towards a relation with macroscopic $|3s_{1/2}^{-1} \otimes 2_1^+(^{130}\text{Sn})\rangle$ configurations.

So one can conclude that the 3 hole shell-model calculation separates in a very distinct way into single-hole configurations and multiplets obtained by coupling single-hole configurations with the $J_i^\pi = 2_1^+$ state in ^{130}Sn . From the theoretical results one also observes rather low-lying high spin states ($J_i^\pi = \frac{23}{2}_1^+$, $E_x = 1.61$ MeV; $\frac{19}{2}_1^+$, $E_x = 1.66$ MeV). As a consequence, isomeric levels can probably occur within the γ decay in ^{129}Sn .

III. APPLICATION TO ODD-MASS AND ODD-ODD Sb NUCLEI

A. Strength of multipole force

In order to perform the shell-model particle core-coupling calculations, as described in Eq.

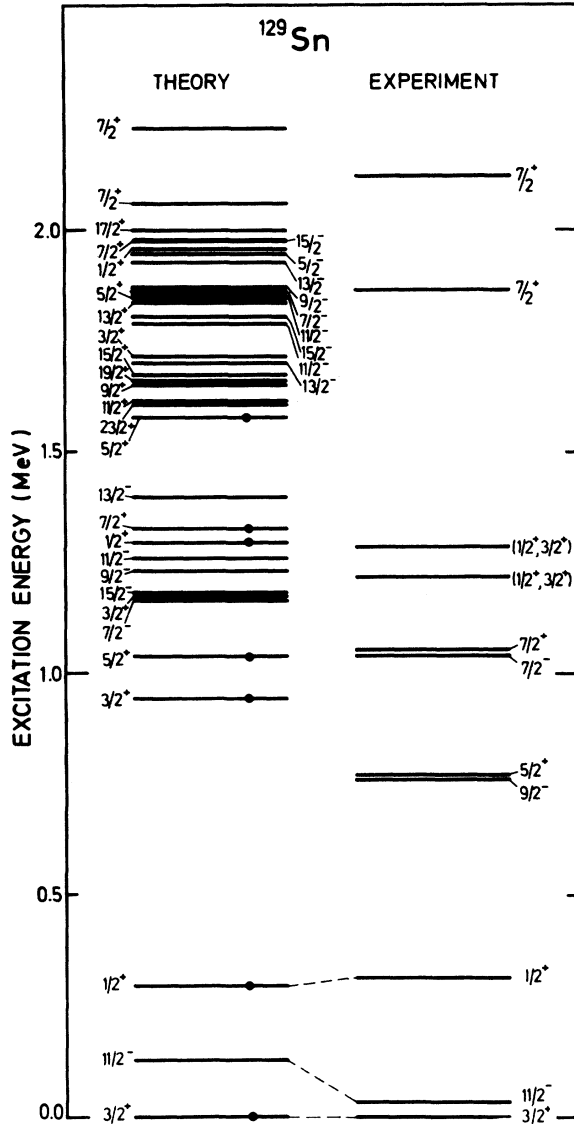


FIG. 1. The 3 hole energy spectrum for ^{129}Sn as compared with the experimental data. Levels marked with a black dot are taken into account for calculating reduced $E2$ core matrix elements as given in Table II.

(2.5), one first has to determine the strengths of the multipole-multipole forces. Moreover, to be able to compare with the purely macroscopic core-coupling calculations where both $\lambda = 2$ and $\lambda = 3$ multipole orders are considered, we take as a residual proton-neutron interaction

$$V_{pn} = \chi_2 Q_2 \cdot Q_2 + \chi_3 Q_3 \cdot Q_3. \quad (3.1)$$

The strengths χ_2, χ_3 will be determined in order to obtain as good an agreement as possible with the experimental data in $^{129}, ^{130}, ^{132}\text{Sb}$. The dependence on χ_2 in all cases is very smooth. In ^{132}Sb the energy separation of the lowest $J^\pi = 4^+$ to 3^+

levels passes through a very flat maximum in the range $\chi_2 = -0.14$ to -0.20 MeV. The same happens in ^{130}Sb . In ^{129}Sb , one can try to fix χ_2 by putting the constraint of reproducing the excitation energy for the two $(\frac{9}{2}, \frac{11}{2})^+$ states at 1.321 and 1.134 MeV. Again, this is possible by choosing a value of $\chi_2 = -0.15$ MeV. Therefore, in all further calculations, we always use $\chi_2 = -0.15$ MeV. In order to study the dependence on χ_3 , we show the 1p-1h, 1p-3h, and 1p-4h spectra (using $\chi_2 = -0.15$ MeV) in Fig. 2. Only those levels which are strongly affected are drawn (relative to the ground state). Thus we present the following remarks.

(i) In the odd-odd nuclei, a particular set of states, mainly originating from the $|1h_{11/2}(\pi), \frac{11}{2}^-(\nu); J^\pi\rangle$ configuration ($J^\pi = 0^+, 1^+, 2^+, 3^+, \dots$), is lowered dramatically with growing χ_3 . This originates from a strong coupling with the higher lying $|2d_{5/2}(\pi)\frac{5}{2}_1^+(\nu); J^\pi\rangle$ configurations due to the very large non-spin-flip $\langle 2d_{5/2} || Y_3 || 1h_{11/2} \rangle$ reduced matrix element.

(ii) In the odd-even nucleus ^{129}Sb , the same happens for the $J^\pi = \frac{5}{2}_1^+$ and $\frac{11}{2}_1^+$ levels due to the same type of coupling matrix element. Here, one can fix χ_3 such as to get the $J^\pi = \frac{5}{2}_1^+$ level on the experimental value, with a result of $\chi_3 = -0.070$ MeV. Using this value, the experimental $(0, 1)^+$ level in ^{130}Sb could correspond with the theoretical $J^\pi = 0_1^+$ or 1_1^+ level.

So we deduce the multipole force with $\chi_2 = -0.15$ MeV and $\chi_3 = -0.070$ MeV to be used in all further calculations.

B. The odd-odd nuclei: $^{132}, ^{130}\text{Sb}$

Using the proton and neutron single-particle energies as already discussed (see also Table I), and using the shell-model particle-core coupling approach, spectra are calculated for the odd-odd nuclei ^{132}Sb (Fig. 3) and ^{130}Sb (Fig. 4). In the particular case of the 1p-1h nucleus ^{132}Sb we also made the comparison with a zero-range residual proton-neutron interaction with spin exchange [$V = -V_1 \delta(\vec{r}_p - \vec{r}_n)(P_s + t'P_\tau)$, see also Table I], as used in Refs. 16 and 17.

Comparing the multipole force with the zero-range force, one observes more closely spaced multiplets in the latter case. Comparing now with experiment,⁵ one cannot prefer one force over the other, since the agreement goes well in both cases. Looking to some more specific details, one recognizes that the $J^\pi = 5^+$ level [mainly $1g_{7/2}(\pi)2d_{3/2}^{-1}(\nu)$] occurs much lower in excitation energy using the δ force as compared to using the multipole force. Also, using the latter force, the lowest negative parity level from the $1g_{7/2}(\pi) - 1h_{11/2}^{-1}(\nu)$ multiplet is not the $J^\pi = 8_1^-$ level as re-

TABLE II. The reduced 3 hole core $E2$ matrix elements, defined as $\langle J_i || Q_2 || J_f \rangle$ for the low-lying ($E_x < 1.5$ MeV) positive parity states (marked with a dot in Fig. 1). The unit is e and the neutron effective charge $e_n^{eff} = 1$ is used. The small line indicates either a nonexistent or a very small (< 0.01) matrix element.

| $J_i^\pi \backslash J_f^\pi$ | $\frac{3}{2}_1^+$ | $\frac{1}{2}_1^+$ | $\frac{3}{2}_2^+$ | $\frac{5}{2}_1^+$ | $\frac{3}{2}_3^+$ | $\frac{1}{2}_2^+$ | $\frac{7}{2}_1^+$ | $\frac{5}{2}_2^+$ |
|------------------------------|-------------------|-------------------|-------------------|-------------------|-------------------|-------------------|-------------------|-------------------|
| $\frac{3}{2}_1^+$ | 0.84 | | | | | | | |
| $\frac{1}{2}_1^+$ | -0.91 | | | | | | | |
| $\frac{3}{2}_2^+$ | -2.22 | 0.84 | -0.66 | | | | | |
| $\frac{5}{2}_1^+$ | -2.77 | -1.22 | 0.23 | -0.70 | | | | |
| $\frac{3}{2}_3^+$ | | 1.90 | 0.07 | 1.10 | 1.77 | | | |
| $\frac{1}{2}_2^+$ | -1.36 | | 1.11 | 0.57 | 0.14 | | | |
| $\frac{7}{2}_1^+$ | 2.19 | | -1.14 | -2.60 | -1.62 | | -0.42 | |
| $\frac{5}{2}_2^+$ | -0.03 | -1.32 | -2.55 | +0.45 | -1.81 | 0.11 | -2.12 | -0.02 |

produced with the δ function interaction.

For $^{130}_{51}\text{Sb}_{79}$, the calculated energy spectrum is compared with experiment⁷ in Fig. 4. A first point stems from the fact that experimentally, the $J_i^\pi = 5_1^+$ level has become the ground state, whereas theoretically no important changes with respect to the 1p-1h system ^{132}Sb occur. Also for the negative parity multiplet $|1g_{7/2}(\pi) \frac{1}{2}_1^-(\nu); J^\pi\rangle$, the sequence as observed experimentally is not reproduced in detail. Since the relative position of the $J_i^\pi = 5_1^+$ and 8_1^+ levels is not known experimentally, we have arbitrarily placed the $J^\pi = 8^-$ level at the same energy as the $J^\pi = 5^+$ positive parity state. Concerning the levels between $0.5 \text{ MeV} < E_x < 1.0 \text{ MeV}$, indeed two theo-

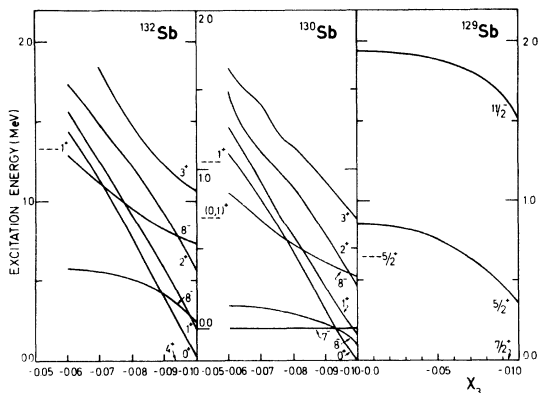


FIG. 2. For the nuclei $^{129,130,132}\text{Sb}$; the dependence on χ_3 only for those levels that are strongly affected by the octupole force. The reference state is $J_i^\pi = 4_1^+$ for ^{132}Sb , $J_i^\pi = \frac{7}{2}_1^+$ for ^{129}Sb , and $J_i^\pi = 7_1^+$ for ^{130}Sb .

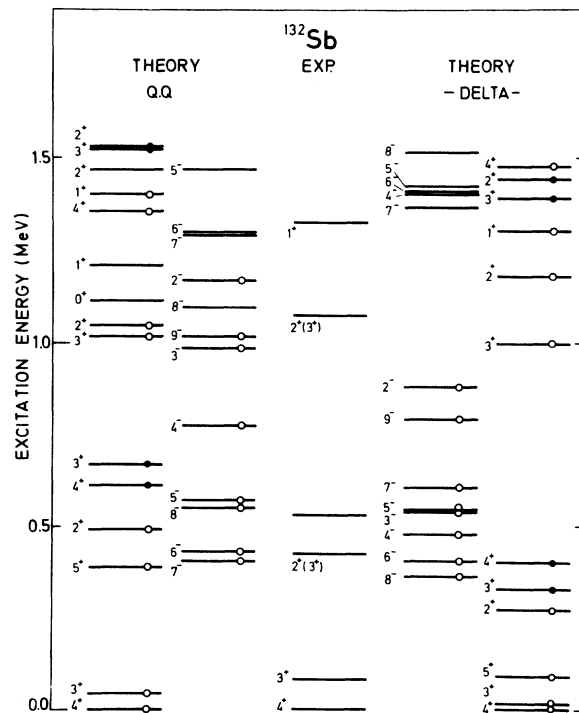
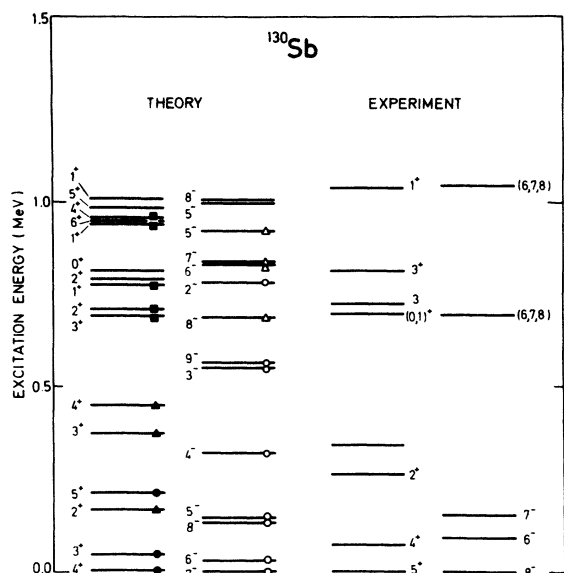


FIG. 3. For the 1p-1h nucleus ^{132}Sb we compare the experimental data with both the results from a delta interaction and a multipole residual proton-neutron interaction. The different multiplets are indicated with, respectively, an open circle [coupling of $1g_{7/2}(\pi)$ or $2d_{5/2}(\pi)$ with $2d_{3/2}(\nu)$, $1h_{1/2}(\nu)$] and a black dot [coupling of $1g_{7/2}(\pi)$ and $2d_{5/2}(\pi)$ with the $3s_{1/2}(\nu)$ configuration].



action.

We now discuss in some detail the similarities and differences between both the macroscopic and shell-model calculations (see wave functions, Tables III-V). Here we would like to point out that the configurations in Tables III-V are labeled according to the shell-model core coupling configurations. These configurations are also used for the macroscopic core coupling wave functions, although in this approach, the corresponding macroscopic quadrupole and octupole configurations, which have a meaning, are marked by an asterisk (see also Ref. 3) (i.e., 2_4^* and 4_1^* correspond with the two quadrupole 2_{2ph}^* and 4_{2ph}^* states, respectively; 3_4^- and 3_5^- both correspond to the single octupole 3_{1ph} state). We can make the following remarks concerning the single-particle states (see Table III).

(i) The $J_i^\pi = \frac{7}{2}^+$ state has about equal single-particle character in both models. The strongest coupling occurs with the $|1g_{7/2}, \frac{7}{2}_1^+\rangle$ configuration in both the shell-model and macroscopic calculations.

(ii) The $J_i^\pi = \frac{5}{2}^+$ level has again comparable single-particle character in both models. For the $|1h_{11/2}, 3^-, \frac{5}{2}^+\rangle$ configuration, about equal admixtures occur, although in the shell-model calculation the coupling with two high-lying $J^\pi = 3^-$ levels occurs preferentially [$|1h_{11/2}, 3_4^-\rangle$ (3.85 MeV) and $|1h_{11/2}, 3_5^-\rangle$ (3.97 MeV); compare the unperturbed energy with $\hbar\omega_3 = 2.9$ MeV in the macroscopic model].

(iii) The $J_i^\pi = \frac{11}{2}^-$ state also has comparable single-particle character in both calculations.

For the $|2d_{5/2}, 3^-\rangle$ configuration, the same comments as for the $J_i^\pi = \frac{5}{2}^+$ level apply.

(iv) For the $J_i^\pi = \frac{3}{2}^+$ levels, some differences occur when comparing both calculations. In the macroscopic calculation the $J_i^\pi = \frac{3}{2}^+$ state is mainly the $|1g_{7/2}, 2_1^+\rangle$ configuration, as is the case also in the shell-model calculation. In the shell-model calculation, a $J_i^\pi = \frac{3}{2}^+$ level occurs, containing as the most important configuration $|1g_{7/2}, 2_2^+\rangle$, a configuration with no counterpart in the macroscopic model.

(v) For the $J_i^\pi = \frac{1}{2}^+$ state, about equal fractions of the $3s_{1/2}$ and the $|2d_{5/2}, 2_1^+\rangle$ configurations result in both descriptions. A second $\frac{1}{2}^+$ level ($J_i^\pi = \frac{1}{2}^+$) is described in the macroscopic model as mainly the $|1g_{7/2}, 4_{2ph}^+\rangle$ configuration, and in the shell-model calculation the corresponding $|1g_{7/2}, 4_1^+\rangle$ configuration dominates.

As a conclusion, we find very strong similarities between both models. For the quadrupole degree of freedom, in both the macroscopic and shell-model descriptions, coupling of the single-particle configuration goes preferentially via the $|nlj, 2_1^+\rangle$ configurations. For the octupole degree of freedom, high-lying $|nlj, 3^-\rangle$ configurations are admixed via the 3_4^- and 3_5^- levels ($E_x = 4.0$ MeV). Also, the strong octupole force dependence is completely analogous in both models due to the large non-spin-flip reduced Y_3 matrix element obtained in both models.

Concerning the one quadrupole $|1g_{7/2}, 2_1^+, J^\pi\rangle$ multiplet, the following points can be made (see Table IV).

(i) The octupole force dependence is very weak

TABLE IV. Comparison of the macroscopic and microscopic wave functions for the levels containing mainly the particle-core coupled $|1g_{7/2}, 2_1^+\rangle$ configuration. The configurations are indicated as $|lj, J_i^\pi\rangle$, where i is the index labeling the levels of the core according to the shell-model description. The asterisk denotes the corresponding macroscopic core states (see also text). The numbers on the right refer to the macroscopic model whereas the numbers to the left give the shell-model particle-core coupling results.

| | $\frac{5}{2}^+$ | $\frac{7}{2}^+$ | $\frac{9}{2}^+$ | $\frac{11}{2}^+$ |
|---------------------|-------------------|-------------------|-------------------|--------------------|
| | $\frac{5}{2}_2^+$ | $\frac{7}{2}_3^+$ | $\frac{9}{2}_4^+$ | $\frac{11}{2}_5^+$ |
| $g_{7/2}^*$ | | -0.31 | 0.30 | |
| $g_{7/2}, 2_1^+$ | 0.84 | -0.95 | -0.62 | 0.87 |
| $g_{7/2}, 2_2^+$ | | | | -0.25 |
| $g_{7/2}, 2_3^+$ | | | | 0.18 |
| $g_{7/2}, 2_4^{+*}$ | -0.28 | -0.42 | 0.18 | -0.30 |
| $g_{7/2}, 3_1^+$ | 0.18 | | | -0.20 |
| $g_{7/2}, 3_2^{+*}$ | | | | 0.30 |
| $g_{7/2}, 4_1^{+*}$ | -0.30 | 0.17 | -0.24 | 0.28 |
| $g_{7/2}, 4_2^+$ | | | | 0.29 |
| $g_{7/2}, 0_2^{+*}$ | | 0.42 | -0.18 | 0.23 |
| $d_{5/2}$ | -0.15 | 0.18 | | 0.17 |

TABLE V. Comparison of the macroscopic and microscopic wave functions for the levels mainly built from particle-core configurations with negative parity core excitations (i.e., $J_i^\pi = 5_1^-, 7_1^-$ mainly). The configurations are indicated as $|lj, J_i^\pi\rangle$, where i is the index labeling the levels of the core according to the shell-model description. The asterisk denotes the corresponding macroscopic core states (see also text). The numbers on the right refer to the macroscopic model whereas the numbers to the left give the shell-model particle-core coupling results.

| | $\frac{9}{2}_1^-$ | $\frac{11}{2}_1^-$ | $\frac{13}{2}_1^-$ | $\frac{15}{2}_2^-$ | $\frac{13}{2}_2^-$ | $\frac{15}{2}_4^-$ | $\frac{19}{2}_1^-$ | $\frac{17}{2}_1^-$ |
|------------------|-------------------|--------------------|--------------------|--------------------|--------------------|--------------------|--------------------|--------------------|
| $g_{7/2}, 7_1^-$ | +0.23 | 0.23 | 0.44 | -0.40 | 0.75 | 0.81 | 0.91 | -0.91 |
| $g_{7/2}, 7_2^-$ | | | -0.28 | -0.24 | | -0.33 | | 0.20 |
| $g_{7/2}, 5_1^-$ | +0.74 | 0.77 | 0.75 | 0.78 | -0.50 | 0.33 | | |
| $g_{7/2}, 5_3^-$ | -0.18 | 0.21 | 0.21 | | | 0.17 | | |
| $g_{7/2}, 6_1^-$ | +0.38 | 0.25 | | -0.26 | 0.17 | | -0.17 | |
| $g_{7/2}, 6_3^-$ | -0.26 | -0.18 | | | | | 0.19 | -0.18 |
| $g_{7/2}, 8_1^-$ | | | | | -0.19 | | 0.23 | |
| $h_{11/2}$ | | 0.29 | | | | | | |
| $d_{3/2}, 7_1^-$ | | | | | | 0.18 | | |
| $d_{3/2}, 7_4^-$ | | +0.18 | | | | | | |
| $d_{3/2}, 6_7^-$ | -0.21 | | | | | | | |
| $d_{5/2}, 5_1^-$ | +0.16 | | | | | | | |

in both models.

(ii) The $|1g_{7/2}, 2_1^*\rangle$ amplitude in all J^π levels ($\frac{3}{2}^+, \dots, \frac{11}{2}^+$) is very large (=0.90).

(iii) The single-particle admixture for the $J_i^\pi = \frac{3}{2}_1^+, \frac{5}{2}_2^+, \frac{7}{2}_3^+$ levels is almost equal in both models.

(iv) In the shell-model approach, the $|1g_{7/2}, 2_1^*\rangle$ configuration couples most strongly with both the $|1g_{7/2}, 4_1^*\rangle$ and $|1g_{7/2}, 2_4^*\rangle$ configurations for the $J_i^\pi = \frac{9}{2}_1^+$ states, a result in agreement with the macroscopic model, where the strongest coupling results for the two quadrupole phonon $|1g_{7/2}, 2_{2ph}^*\rangle$ and $|1g_{7/2}, 4_{2ph}^*\rangle$ configurations.

Now for the $|1g_{7/2}, 7_1^-\rangle$ and $|1g_{7/2}, 5_1^-\rangle$ configurations, negative parity multiplets result that are not easily obtained in the macroscopic model (see Table V).

IV. CONCLUSION

In this study, we have proposed a shell-model approach to particle-core coupling near closed-shell configurations. We first performed a shell-model treatment of the core nuclei with 2 hole, 3 hole, 4 hole configurations (exactly). Going beyond will need certain approximations such as taking only the lowest 0^+ and 2^+ 2 hole states acting on the 4 hole spectrum; in producing 6 hole, 8 hole, ... configurations.

In describing the most simple core nuclei (2h, 3h, 4h) we obtain results in good agreement with

the generalized seniority classification of N particles (- holes) distributed over a number of degenerate j shells, i.e., the vibrational spectrum of double-even nuclei is obtained. (see also Ref. 3). Reduced core $E2$ matrix elements, resembling very much the quadrupole boson cfp values (although anharmonicities do play an important role) also result. The general expression (2.5) has been obtained and applied to odd-odd as well as to odd-even nuclei. Application was made to $^{129,130}\text{Sb}$ and ^{132}Sb where, in the former case, extensive comparison with the macroscopic particle core coupling model is carried out. Here, we obtain a description of the experimental data which is as good as that for the macroscopic model. Moreover, due to the shell-model description of the core system, all types of more complex particle-core coupled configurations can result which are not at all considered in the purely macroscopic approach.

Therefore, the method discussed here can serve as a shell-model version of the macroscopic particle-core coupling model, being able to extend the limit of validity to excitations not easily obtained in the latter model.

ACKNOWLEDGMENTS

The authors are most grateful to Prof. R. Chéry and Prof. A. J. Deruytter for their interest during the course of this work. One of the authors

(K. H.) is very much indebted to Prof. R. Chéry for hospitality during his stay at the IPN, Lyon, and to the I N2 P3 for financial support. We also

owe much to discussions and communications with B. Fogelberg, K. Sistemich, F. Schussler, B. Walters, and R. A. Meyer.

*Permanent address: Institute for Nuclear Physics, Proeftuinstraat 86 B-9000 Gent, Belgium.

¹E. Lund, K. Aleklett, and G. Rudstam, Nucl. Phys. A286, 403 (1977).

²K. Aleklett, E. Lund, and G. Rudstam, Phys. Rev. C 18, 462 (1978).

³B. Fogelberg, K. Heyde, and J. Sau, Nucl. Phys. A352, 157 (1981).

⁴C. E. De Geer and G. B. Holm, Phys. Rev. C 22, 2163 (1980).

⁵A. Kerek, G. B. Holm, P. Carlé, and J. McDonald, Nucl. Phys. A195, 159 (1972).

⁶K. Heyde, J. Sau, R. Chéry, F. Schussler, J. Blachot, J. P. Bocquet, E. Monnard, and K. Sistemich, Phys. Rev. C 16, 2437 (1977).

⁷A. Kerek, P. Carlé, and S. Borg, Nucl. Phys. A224, 367 (1974).

⁸R. L. Auble, J. B. Ball, and C. B. Fulmer, Nucl. Phys. A116, 14 (1968).

⁹F. Schussler, J. Blachot, J. P. Bocquet, and E. Monnard, Z. Phys. A 281, 229 (1977); private communication.

¹⁰J. McDonald and A. Kerek, Nucl. Phys. A206, 417

(1973).

¹¹A. Kerek, G. B. Holm, S. Borg, and P. Carlé, Nucl. Phys. A209, 520 (1973).

¹²K. Sistemich, W. D. Lauppe, T. A. Khan, H. Lawin, H. A. Selic, J. P. Bocquet, E. Monnard, and F. Schussler, Z. Phys. (to be published).

¹³J. Sau and K. Heyde, Phys. Rev. C 21, 419 (1980).

¹⁴J. Sau, K. Heyde, and M. Waroquier, Nucl. Phys. A298, 93, (1978).

¹⁵J. Sau and K. Heyde (unpublished).

¹⁶P. Van Isacker, K. Heyde, M. Waroquier, and H. Vincx, Phys. Rev. C 19, 498 (1979).

¹⁷J. Sau, K. Heyde, and R. Chéry, Phys. Rev. C 21, 405 (1980).

¹⁸K. Heyde and M. Waroquier, Nucl. Phys. A167, 545 (1971).

¹⁹M. Waroquier and K. Heyde, Nucl. Phys. A164, 113 (1971).

²⁰M. Waroquier and K. Heyde, Z. Phys. 268, 11 (1974).

²¹S. Sen and B. K. Sinha, Nucl. Phys. A157, 497 (1970).

²²G. Vanden Berghe and K. Heyde, Nucl. Phys. A163, 478 (1971).